

CHROM. 16,401

## DETERMINATION OF BAND-SPREADING EFFECTS IN HIGH-PERFORMANCE LIQUID CHROMATOGRAPHIC INSTRUMENTS\*

K.-P. HUPE\*, R. J. JONKER and G. ROZING  
*Hewlett-Packard GmbH, 7517 Waldbronn-2 (F.R.G.)*  
(Received September 22nd, 1983)

---

### SUMMARY

The fundamentals of the measurement and computation of band spreading generated in chromatographic systems are discussed. A computer program was written that allows the characterization of the dispersion effects by calculating the second statistical moment of the concentration profiles emerging from the system. Experimental determination is necessary, as the existing theoretical models give quantitatively accurate values only in certain instances. In this way the dispersion contributions of various system elements were determined and useful hints for their design were obtained.

---

### INTRODUCTION

The recent trend in liquid chromatography towards smaller columns with respect to both length and diameter, the still improving efficiency of column packing materials and the desire for an increased speed of analysis have intensified the demands on the chromatographic system with respect to its dead volume and band spreading contribution.

In this context, a review showing how the band-spreading contribution of available columns and that of available liquid chromatographic systems have developed over the years is of interest. The middle line in Fig. 1 shows the band spreading within the column and is determined by points 1, 2 and 3, which are taken from the literature<sup>1-3</sup>. Point 1 stems from one of the very first papers on high-performance liquid chromatography (HPLC), where a column having a length of 1 m and a diameter of 4 mm filled with brickdust of 100-120 mesh (0.125-0.136 mm) was investigated. The measured plate height for an early eluting peak was 1 mm and its volume standard deviation was almost 300  $\mu$ l. Since then column development has made remarkable progress, so that today high-efficiency columns are available, the dispersion of which has a volume standard deviation of no more than 5-15  $\mu$ l for early eluting peaks. Point 3 has been taken from two fairly recent publications, one where

---

\* Presented at the symposium *Columns in High-Performance Liquid Chromatography*, Cambridge, September 22-23, 1983.

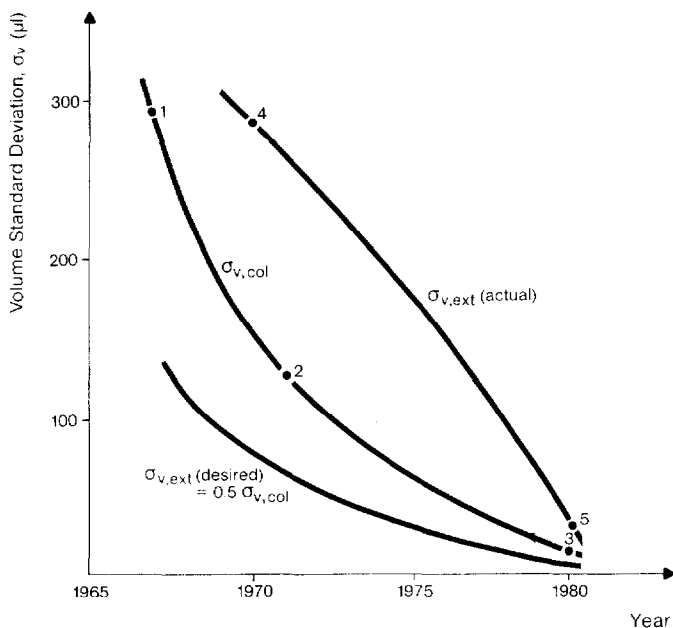


Fig. 1. Band spreading inside and outside HPLC columns.

HPLC columns were investigated under high-speed conditions<sup>3</sup> and the other on micro-bore columns with very low flow-rates<sup>4</sup>.

It has always been regarded as a good objective to design chromatographic instruments so that the dispersion in the system outside the column would not destroy more than 10% of the resolution achieved within the column. As a consequence, the external band spreading expressed as the peak standard deviation must be less than 50% of that of the column. This desired value is represented by the lower line in Fig. 1.

The actual external dispersion, as it has developed over the years, is shown qualitatively by the upper curve in Fig. 1. Point 4 is a value recalculated from an instrument (in the design of which one of the authors has participated) at a time when the typical inner diameter of the connecting lines had just been changed from 0.5 to 0.3 mm. Point 5 is taken from two more recent publications<sup>3,4</sup>.

One can see a large difference between the actual and the desired values for the external band spreading, a discrepancy for which the manufacturers of HPLC equipment have often been criticized. Only in recent years has this gap been closed and now there are commercially available instruments with a total external band-spreading contribution of not more than 3–5  $\mu\text{l}$  expressed as volume standard deviation.

There are strong arguments for decreasing this value even further, possibly below 1  $\mu\text{l}$ . This is certainly possible, but will be extremely difficult to realise if the signal-to-noise ratio of present detectors is to be maintained and if instruments with these specifications are still to offer a certain versatility and are still to be used for routine purposes.

It appears today that the question of what will ultimately be the lowest column

diameter for practical use will not be answered by suitable column packing techniques but by the ability to design chromatographic equipment with an appropriately small band-spreading contribution.

#### METHOD OF MEASUREMENT

A reduction to 1–5  $\mu\text{l}$  in the volume standard deviation for the external band spreading puts severe demands on the measurement of this phenomenon. This is true particularly if one is interested not only in the overall dispersion of the total system but also in that of the various subsystems, including injection device, connecting elements, column end fittings and detector cell, and the response behaviour of the electronic parts of the detector and the data acquisition system.

Practical measurements can be carried out with or without a column in the system. In the first method, the variances of a series of consecutive peaks, measured in time units, are plotted against the square of their retention times. After linear regression, the variance of the external band spreading is obtained as the intercept at retention time zero. This method has been used by Lauer and Rozing<sup>14</sup> to investigate the effect of the injection volume on external band spreading. Although elegant, this method has limitations (dependence on substances) and is time consuming.

The other method, which has been applied in this investigation, measures the dispersion of the external system directly. The column is replaced by a fitting of zero dead volume. The problem here is that the concentration profiles to be determined are very fast. Most of the measurements have to be carried out in less than 1 sec, requiring extremely small time constants of the detector electronics combined with a high data acquisition rate.

The system that we used had an overall time constant of 50 msec for the detector electronics and data acquisition system and a data acquisition rate of 16 Hz. The contribution due to the electronic time constant is between 0 and 3  $\mu\text{l}$  volume standard deviation, depending on the flow-rate. This value, however, is known and constant so that the measurements can be corrected for it.

These specifications provide a precision of better than 5% (standard deviation) for at least five measurements which have been conducted for every data point shown in the figures.

The dispersion was determined by calculating the second statistical moment of the concentration profiles emerging from the system, according to eqn. 1 and Fig. 2.

$$M_2 = \sigma_t^2 = \frac{\int_{t_B}^{t_E} (t - M_1)^2 c(t) dt}{\int_{t_B}^{t_E} c(t) dt} \quad (1)$$

where  $t$  = time;  $t_B$  = beginning of integration;  $t_E$  = end of integration;  $c(t)$  = concentration as function of time;  $M_0$  = zeroth statistical moment (area under concentration profile);  $M_1$  = first statistical moment (centre of gravity); and  $M_2$  = second statistical moment (time variance).

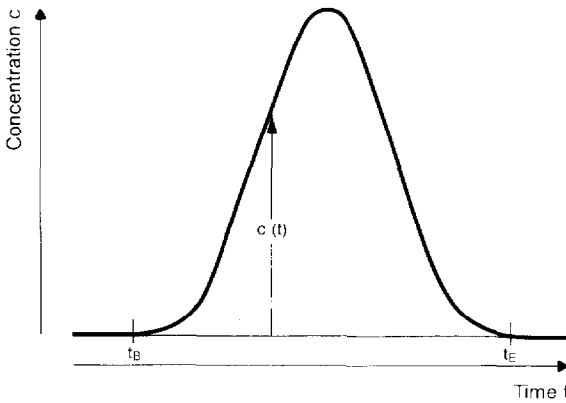


Fig. 2. Characterization of concentration profile by second central moment.

The calculations were carried out on an HP 1000 computer, for which a Basic program had been written (memory requirements for peak recognition and calculation of the first three moments, 80 kbytes; calculation time, 3 min).

To be able to compare the results obtained with those in the literature using standard deviations based on graphical determination of the half-width from recorder traces, a computer program was written that simulates this method. According to Fig. 3, this program determines the "standard deviation" of a concentration profile by taking the half-width at 60.7% of the maximum.

As stated by various authors<sup>5,6</sup> and as will also be shown in this work, graphically determined standard deviations are not suitable as a measure of external band spreading. Their application implies a Gaussian concentration profile. Profiles generated outside the column, however, are exponential and highly unsymmetrical. Graphically determined standard deviations therefore give results that are generally too low by 100–200%. In addition, they do not properly show the dependence of band spreading on parameters such as flow-rate, capacity factor or injection volume, where the relative magnitude of various modifiers change during the experiment.

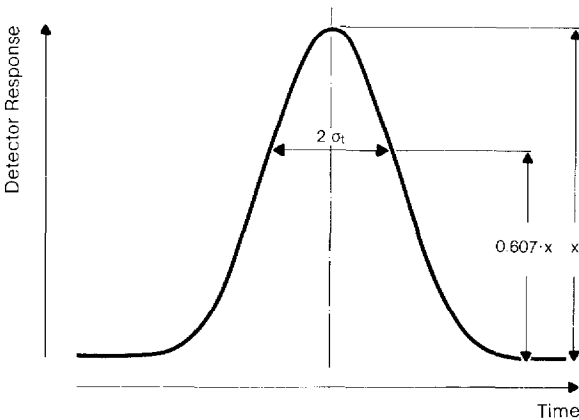


Fig. 3. Characterization of a peak by "half-width method".

Moreover, they do not permit addition or subtraction of the variances of various subsystems. All these mistakes can, however, be omitted by applying properly calculated second moments.

### THEORETICAL CONSIDERATIONS

A concentration profile passing through a flow system is modified by every system element. Mathematically, an input function is modified by the pulse function (of a subsystem) to give the output function (Fig. 4). With the input and the response function known, the output function can be calculated by solving the convolution integral<sup>5</sup>. This is possible for simple and/or idealized situations only. For our purposes it is helpful to know the variances of the individual functions because the variances of the input and of the response function (if independent from each other) can be added, to give the variance of the output function. This means that the variance of the response functions of all subsystems can be added to give the variance of the total system.

Table I lists the most important dispersion sources occurring in a liquid chromatographic system. Apart from the column and the sample itself, laminar flow profiles and dead volumes are the dominant contributors to band spreading. In fast analyses, the time constant of the electronic system also contributes. Column 2 in Table I shows the corresponding response functions and column 3 their second moments, expressed as the volume-based variance. Column 4 indicates the amount of proportionality to flow.

When applying the expressions for the second moments to practical cases, it must be borne in mind that they refer to simplified models. Only in certain instances, therefore, can these expressions be used to determine the dispersion of a system element in a quantitatively correct way. In general, however, a more or less great departure between the model and reality will be noticed.

On the other hand, the qualitative dependence of the dispersion effects on the various parameters, especially diffusion coefficient and flow-rate, will be preserved, and a knowledge of these coherences can be very helpful for the interpretation of experimental results. Knowing that the variance of the total system is made up of the variances of the subsystems may be used subsequently to identify the various subsystems and their dispersion behaviour. Both strategies, which have already been

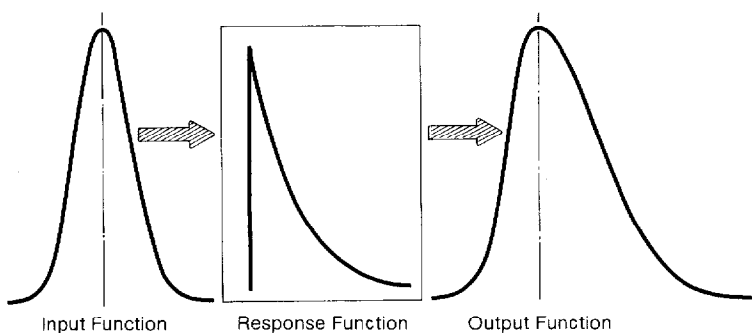







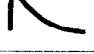


Fig. 4. Modification of a concentration profile in a flow system.

TABLE I  
SOURCES OF ZONE DISPERSION IN CHROMATOGRAPHIC SYSTEMS

Symbols:  $A$ , capillary cross-section;  $F$ , solvent flow-rate;  $D$ , diffusion coefficient;  $L$ , capillary length;  $V_{inj}$ , injection volume;  $V_M$ , dead volume;  $x$ , characteristic length;  $a'$ ,  $b'$ ,  $c'$ ,  $C$ ,  $D$  and  $E$ , constants;  $\sigma_v^2$ , volume variance of response function;  $\tau$ , time constant.

Source of dispersion	Response function	Second moment, $\sigma_v^2$ ( $\mu^2$ )	Flow dependence, $F$ ( $\mu\text{l}/\text{sec}$ )	Remarks	Ref.
Column		$a' + \frac{b'}{F} + c'F$	$F$ (dominant)	Van Deemter eqn.	7
Sample		$\frac{V_{inj}^2}{12}$	—	—	5
Poiseuille flow + radial diffusion		$\frac{LA^2F}{\pi \cdot 24D}$	$F$	Valid only for straight tubes of certain length	8-12
Longitudinal diffusion		$\frac{2DLA^3}{F}$	$\frac{1}{F}$	Negligible in LC	11
Dead volume (convection controlled)		$V_M^2$	—	Perfect mixer	5
Dead volume (diffusion controlled)		$\frac{x^4 F^2}{4D}$	$F^2$	—	5
Laminar flow + inertial flow + radial diffusion		$E(BF - CF^5)$	$E(BF - CF^5)$	—	13
Electronic response delay		$\tau^2 F^2$	$F^2$	—	5

suggested by Sternberg in his fundamental work in 1966<sup>5</sup>, have been applied in this work.

## EXPERIMENTAL

The experiments were carried out with a Hewlett-Packard 1084B liquid chromatograph. Second moments of emerging concentration profiles were calculated by the described computer program. Each point in the figures is the mean value of at least five measurements, the standard deviation of which was always smaller than 5%. The flow-rate was measured volumetrically and was always in close agreement with the value indicated by the instruments flow measuring system.

Water-acetonitrile (60:40) was used as the eluent, into which 1  $\mu\text{l}$  of diethylphthalate (0.05%, v/v, dissolved in the eluent) was injected.

Fig. 5 shows a plot of the second moment *versus* flow-rate for a system consisting only of a Rheodyne injection valve with a 1- $\mu\text{l}$  sample loop and a 4.5- $\mu\text{l}$  flow cell of a variable-wavelength UV detector, both connected by a steel capillary and a fitting of zero dead volume, as indicated. In the following discussions this system will be referred to as the "basic system".

In order to obtain an idea of the accuracy of the method, a source of known dispersion was added to the basic system as shown in Fig. 6. This was a straight

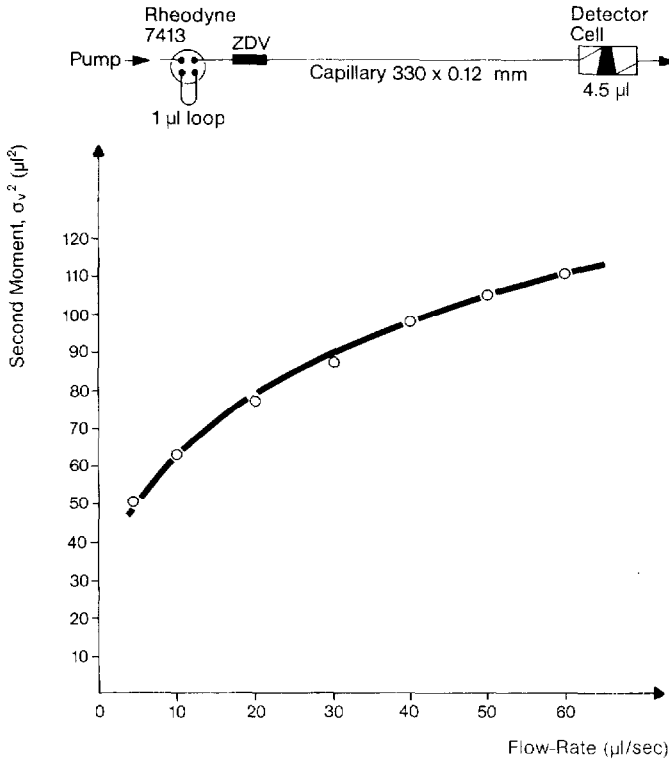


Fig. 5. Second moment,  $\sigma_v^2$ , versus flow-rate for the basic system.

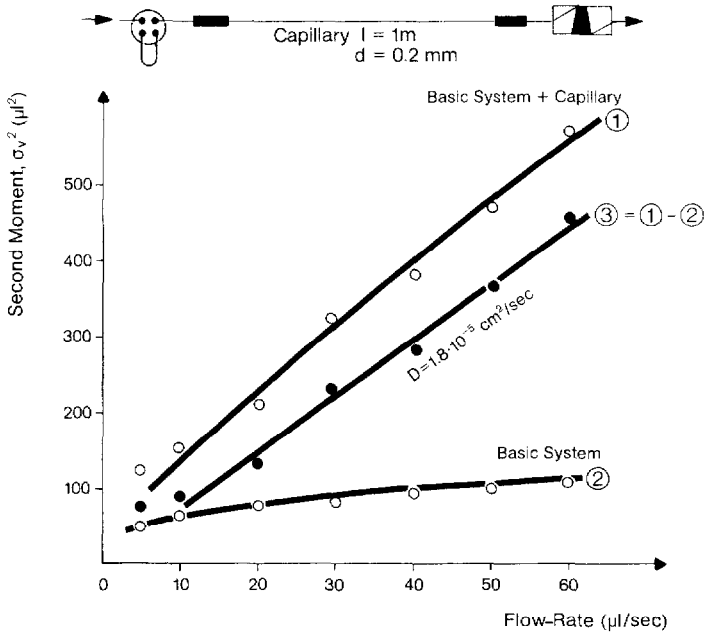


Fig. 6. Second moment,  $\sigma_v^2$ , versus flow-rate for the basic system extended by a capillary.

capillary with a length of 100 cm and an inner diameter of 0.2 mm. The dispersion of this capillary, according to Atwood and Golay<sup>12</sup>, can be described by the Taylor equation<sup>8,9</sup>. Simultaneously the question of whether the variances of the response functions of the basic system and of the capillary were additive should be answered.

The upper line (1) in Fig. 6 shows the second moment for the basic system extended by the straight capillary. From these values those for the basic system (2) were subtracted to give curve (3), isolating the dispersion contribution of the capillary. As the Taylor equation predicts, this is a straight line passing through the origin. At low flow-rates a deviation of the measured values from the straight line was observed which could not be explained. The diffusion coefficient of  $D = 1.8 \cdot 10^{-5}$  cm<sup>2</sup>/sec which belongs to that line is in accordance with values given in the literature. The results show that the measurements are in good accordance with theoretical predictions with respect to both the Taylor equation and the additivity of second moments.

The same method was now applied in an attempt to explain the course of the plot for the basic system. The dominant subsystems here are the injection valve, the detector flow cell and the connecting elements. In order to isolate the influence of the detector cell, another flow cell, identical with that of the basic system, was added to the basic system and the overall variance measured as a function of flow-rate. Fig. 7 again shows the curve for the basic system (2) and that for the basic system extended

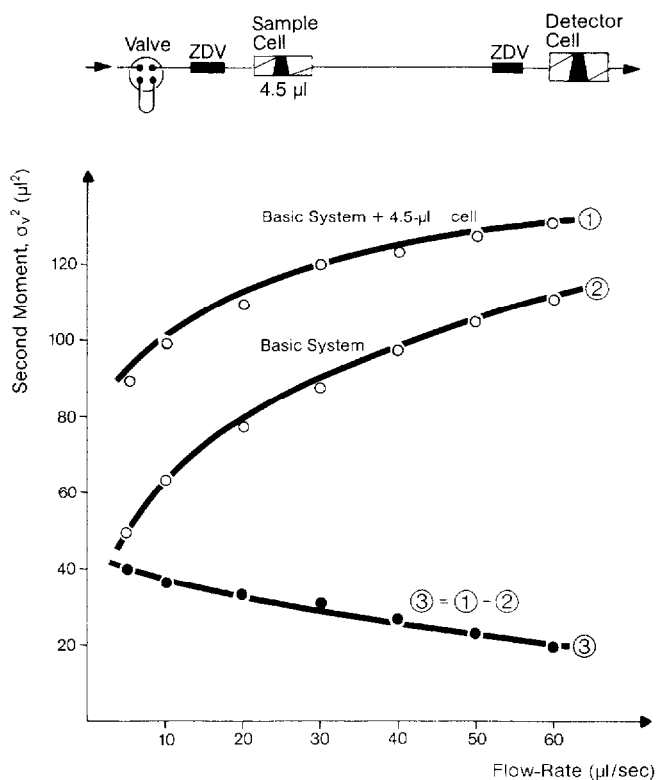


Fig. 7. Second moment,  $\sigma_v^2$ , versus flow-rate for the basic system extended by a 4.5- $\mu l$  flow cell.



by a 4.5- $\mu\text{l}$  flow cell (1). The curves were subtracted from each other, giving the curve for the dispersion contribution of the flow cell (3).

Before any conclusions were drawn, a second flow cell, larger but having the same geometry, was measured in the same way. The result is shown in Fig. 8, together with the curve for the 4.5- $\mu\text{l}$  cell in Fig. 7. The shape of the curves suggests that at low flow-rates, a laminar flow profile exists, which obviously is destroyed by secondary flow with increasing velocity. The results simultaneously indicate that the main contribution to dispersion in the basic system cannot be attributed to the flow cell but is obviously generated by the injection system. Hence there is evidence that the impact of the eluent on the sample at the moment of injection, accelerating the sample plug from zero to a speed of 5 m/sec in a very short time, causes the observed dispersion.

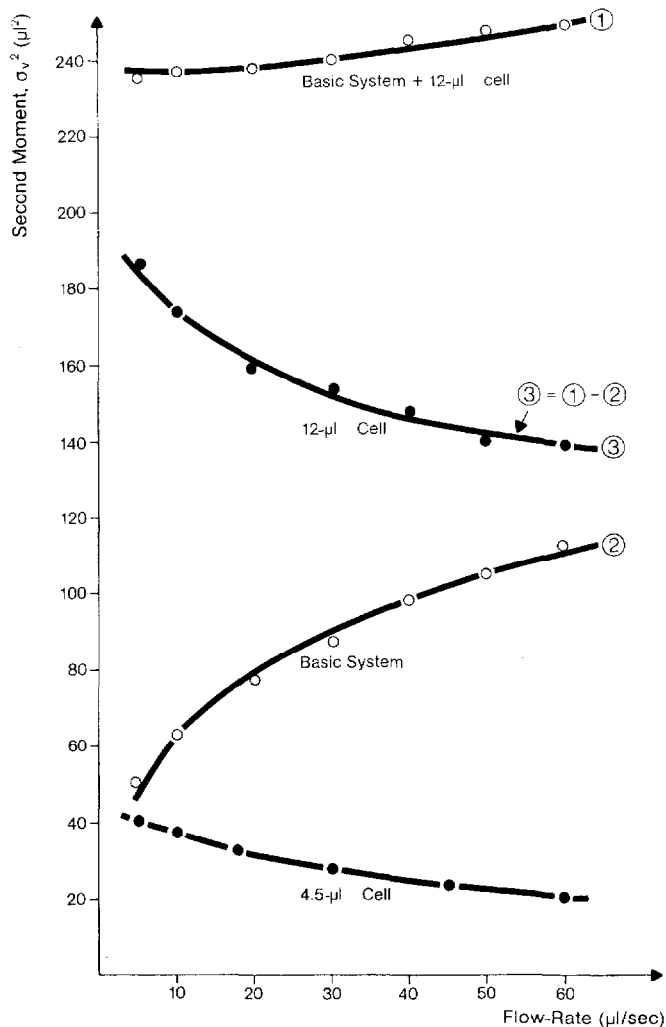


Fig. 8. Second moment,  $\sigma_v^2$ , versus flow-rate for the basic system extended by 12- $\mu\text{l}$  flow cell.

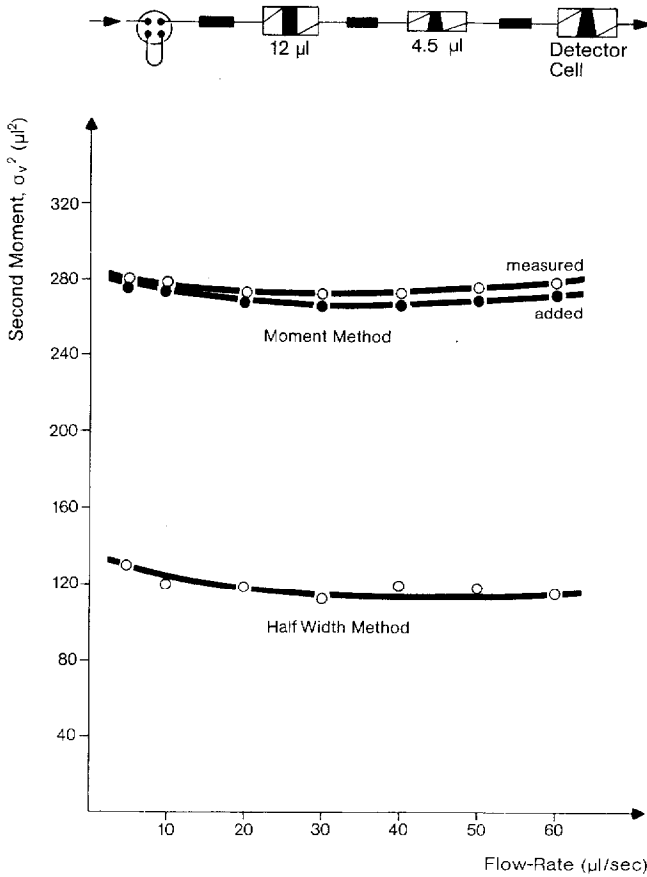


Fig. 9. Second moment,  $\sigma_v^2$ , versus flow-rate measured and added for the basic system and two flow cells.

The measurements on the two flow cells were used again to check the additivity of the variances. For this purpose both cells were added to the basic system and the overall second moment was measured as a function of the flow-rate. These values were compared with those derived by adding the second moments of the isolated cells and the basic system. Fig. 9 shows that both results are in good accordance, demonstrating that properly measured second moments can be added and subtracted from each other.

The upper curve in Fig. 9, presenting second moments, was compared with values derived by applying the graphical method for the determination of the peak half-width (see the lower line in Fig. 9). As already mentioned, these values are far too low (by a factor of 2-3) and do not represent the proper dependence of dispersion on flow-rate. With increasing flow-rate, the profiles show an increasing skew, which is not taken into account by determining the peak half-width.

A  $100 \times 4.6$  mm I.D. column packed with ODS-Hypersil ( $5 \mu\text{m}$ ) was added to the basic system. For these measurements  $2 \mu\text{l}$  of a mixture of thiourea and phenol, both diluted in the solvent, were injected. Thiourea has a capacity factor of about zero while that of phenol is 1.3. The apparent plate height was now calculated from

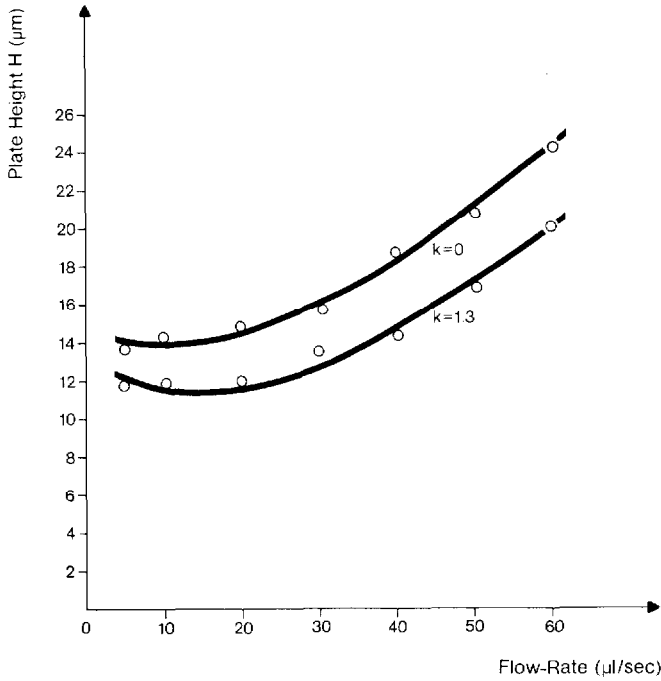


Fig. 10. Van Deemter plot of apparent plate height.

the acquired data. This is part of the computer program. The plots of the obtained values *versus* flow-rate (Fig. 10) show a strong dependence on the capacity ratio ( $k$ ).

Second moments were determined as before and are plotted in Fig. 11. Both curves were then corrected for the measured dispersion of the basic system. From the

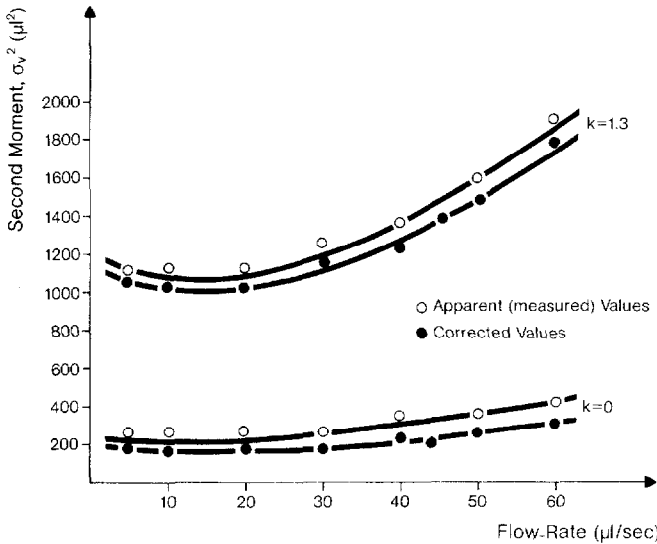


Fig. 11. Second moment,  $\sigma_v^2$ , *versus* flow-rate for basic system + column.

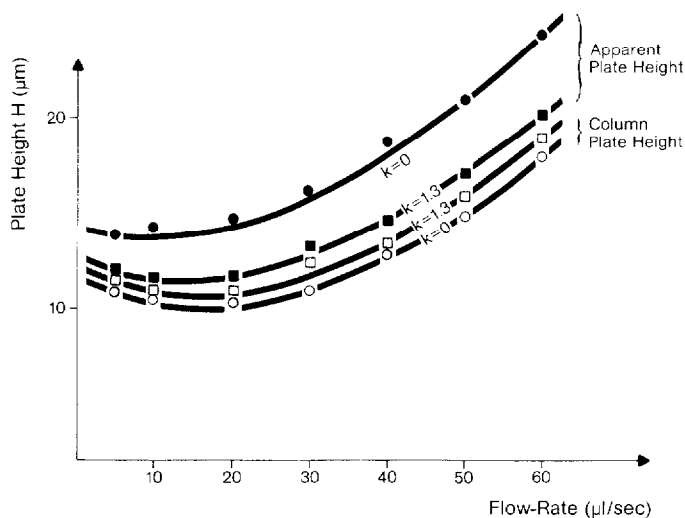


Fig. 12. Van Deemter plot of apparent and corrected plate height.

corrected values the theoretical plate height ( $H_0$ ) was calculated using the equation

$$H_0 = l \frac{\sigma_{v_{col}}^2}{V_R^2} \quad (2)$$

where  $l$  is column length,  $V_R$  is retention volume and  $\sigma_{v_{col}}^2$  is volume variance of the column after correction for external contribution. The values are shown in Fig. 12, together with the apparent plate height. It now becomes evident that the strong dependence on the capacity ratio is due to the dispersion of the external system: its band-spreading effect influences the early eluting peaks much more than those having higher  $k$  values. The corrected plate height shows the dispersion of the column only. The dependence on the capacity factor has become very small, with the values for the lower capacity ratio lying below those of the higher, as one would expect from theory. At the optimal flow-rate of about 20  $\mu\text{l}/\text{sec}$  (1.2 ml/min), the reduced plate height has a value of about 2.

## CONCLUSION

We have presented an empirical method that allows the characterization of the dispersion behaviour of individual chromatographic subsystems as a function of the flow-rate. As flow is indispensable in HPLC and as a non-separating volume in the system is inevitable, we suggest that any instrument be characterized by a  $\sigma_v^2$  versus flow-rate curve, by analogy with the Van Deemter curve of a column. This curve, of course, can only be obtained properly if variances are calculated as their second, central, normalized moment.

With our basic system, under the prerequisite of adequate real-time registration of the profiles, we have determined by the addition of subsystems their individual contributions. The results show that well designed flow cells at flow-rates higher than

50  $\mu\text{l}/\text{sec}$  behave as ideal mixers, generating a variance equal to the square of the cell volume, independent of flow-rate.

This led to the presumption that the major source of external band spreading in the basic system at higher flow-rates is the injection procedure. We postulate the excessive acceleration of the sample to be responsible for this, a point which, however, has to be clarified by further experiments.

If variances are properly calculated, they do add as expected, within experimental error.

In this low diluting system, even relatively high-volume columns (100  $\times$  4.6 mm I.D.) still suffer with low  $k$  values from external band spreading. Only if this is accounted for can true column efficiencies, close to the theoretical limit, be obtained.

#### REFERENCES

- 1 R. P. W. Scott, D. W. J. Blackburn and T. Wilkins, *J. Gas Chromatogr.*, (1967) 183.
- 2 R. P. W. Scott and P. Kucera, *J. Chromatogr. Sci.*, 9 (1971) 641.
- 3 J. L. DiCesare, M. W. Douy and L. S. Ettre, *Chromatographia*, 14 (1981) 257.
- 4 R. P. W. Scott and P. Kucera, *J. Chromatogr.*, 169 (1979) 51.
- 5 J. C. Sternberg, *Advan. Chromatogr.*, 2 (1966) 205.
- 6 J. J. Kirkland, W. W. You, H. J. Stoklosa and C. H. Dilks, Jr., *J. Chromatogr. Sci.*, 15 (1977) 303.
- 7 J. J. van Deemter, F. J. Zuiderweg and A. Klinkenberg, *Chem. Eng. Sci.*, 5 (1956) 271.
- 8 G. Taylor, *Proc. R. Soc. London, Ser. A*, 219 (1953) 186.
- 9 G. Taylor, *Proc. R. Soc. London, Ser. A*, 225 (1954) 473.
- 10 A. Aris, *Proc. R. Soc. London, Ser. A*, 235 (1956) 67.
- 11 M. J. E. Golay, in D. H. Desty (Editor), *Gas Chromatography 1958*, Academic Press, New York, 1958, p. 36.
- 12 J. G. Atwood and M. J. E. Golay, *J. Chromatogr.*, 218 (1981) 97.
- 13 M. J. E. Golay, *J. Chromatogr.*, 186 (1979) 341.
- 14 H. H. Lauer and G. P. Rozing, *Chromatographia*, 14 (1981) 641.